



A deep neural network and machine learning approach for retinal fundus image classification

Rohit Thanki

Krian GmbH, Wolfsburg, Germany

ARTICLE INFO

Keywords:

Classification
Deep neural network
Glaucoma
Retinal image
Machine learning

ABSTRACT

Diabetes is a common chronic disease and a major public health problem approaching epidemic proportions globally. People with diabetes are more likely to suffer from glaucoma than people without diabetes. Glaucoma can lead to loss of vision if not diagnosed at an early stage. This study proposes an intelligent computer-aided triage system with a deep neural network and machine learning to develop and analyze color retinal fundus images and classify glaucomatous retinal images. Deep features of retinal images from the fundus retinal image are extracted using a deep neural network, and the classification of features is performed and analyzed using different machine learning classifiers. Experimental results show that the combination of deep neural network and logistic regression-based classifier outperforms all existing glaucomatous triage systems, improving classification accuracy, sensitivity, and specificity.

1. Introduction

According to the World Health Organization (WHO) report [1], glaucoma is one of major eye disease which is affecting millions of people in developing countries such as India. The Glaucoma damages the retina in a progressive manner and is less detected by the person and finally causes blindness. As per the survey of glaucoma society of India [2], around 12 million people in India are suffering from this disease. Therefore, early detection and treatment of glaucoma to reduce the risk of blindness is the need of the hour. The acquisition of retinal information of eye is usually performed by gonioscopy and ophthalmoscopy. Then, the analysis of glaucoma for physical condition of the optical nerve is done by filed vision test, intraocular pressure, etc. [3–5]. The glaucoma detection can be performed using optical coherence tomography (OCT), visual test chart and color fundus camera. The glaucoma detection can also be done by analyzing features such as cup-to-disk (CDR) and disk rim thickness rule of inferior, superior, nasal, and temporal (ISNT).

Recently, computer-aided systems [6–18] based on various image processing and machine learning algorithms are gaining importance for intelligent detection of glaucoma [19,20]. While supervised machine learning algorithms are used for classification of the normal image and glaucomatous image for a given dataset of the retinal image, the unsupervised machine learning algorithms are used mainly for segmentation of disk and cup in the enhanced retinal image. Recently, the various schemes are proposed by various researchers for detection of glaucoma in retinal images.

Claro et al. [6] performed classification of retinal images using classifiers such as the multi-layer perceptron (MLP), random forest (RF) and

radial basis function (RBF) on the DRISTHI-GS1 dataset and obtained accuracy in the range of 83.54–93.03%. Another automated glaucoma screening system developed by Soman et al. [7] used wavelet features of retinal images and performed classification of high-resolution fundus retinal images using classifiers such as SVM, RF, NB and resulted in accuracy of 85.65%, 86% and 81%, respectively. Dey et al. [8,13] used statistical features for development of an automated glaucoma screening system for retinal image classification using SVM classifier. Maheshwari et al. [9] developed glaucoma screening system for classifying glaucomatous retinal images with an accuracy of 98.33%, taking wavelet and corr-entropy of retinal images as features.

Singh et al. [10] developed glaucoma screening system for classifying glaucomatous retinal images from the Technische Fakultat dataset with accuracy in the range of 92%–97% with KNN, naïve bayes and SVM classifier. Sevastopolsky et al. [11] developed glaucoma screening system for classifying glaucomatous retinal images from the DRISTHI-GS1 dataset using SVM classifier. Sarkar et al. [12] developed glaucoma screening system for classifying glaucomatous retinal images from the RIM-ONE dataset using binary classifier with an accuracy of 97.58%.

Nawaldgi et al. [14] used DRISTHI-GS1 dataset with binary classifier and achieved an accuracy of 99%. Septiarini et al. [15] developed glaucoma screening system based on supervised learning for classifying retinal images and the accuracy resulted with naïve bayes, MLP, SVM, and kNN is in the range 92.90%–95.12%. Zou et al. [16] used SVM and random forest on the DRISTHI-GS1 dataset and achieved accuracy in the range 74%–78%. Yip et al. [17] give analysis of various deep learning (DL) models for diabetic retinopathy. They used various

E-mail address: rohitthanki9@gmail.com.

<https://doi.org/10.1016/j.health.2023.100140>

Received 30 September 2021; Received in revised form 31 December 2022; Accepted 16 January 2023

models such as VGGNet, ResNet, DenseNet and Ensemble for analysis. For detection of DR, four DL models showed comparable diagnostic performance using AUC in range of 0.936 to 0.944. Sahlsten et al. [18] proposed AI based model for diabetic retinopathy using fundus retinal images. They are used around 41,122 retinal color images from 14,624 patients for analysis of deep learning model. The inception V3 model used and provides sensitivity up to 0.968 (0.961–0.974) and specificity up to 0.893 (0.883–0.902). Wang et al. [21] demonstrated transfer learning models for classification of retinal image classification.

Gupta et al. [22] proposed optimal learning model for retinal image classification. In this system, authors used two filters such as guided filter and adaptive median filter for preprocessing of images before fed to neural network. The features of images are extracted using efficient network feature extractor while mayfly optimization with kernel-based machine learning model used for classification of images. Abdel-Hamid [23] proposed VGG16 transfer learning-based model for classification of retinal image. This approach is used for quality checking of retinal image before used for further applications. Goel et al. [24] proposed VGG based deep learning model for classification of various stages of diabetic retinopathy using retinal images. Kaur et al. [25] proposed k-nearest neighbor-based classifier system for retinal image classification. This system used for classification of diabetic retinopathy retinal images and used wavelet features of images for classification of images. Saba et al. [26] proposed triage system with help of two deep learning models for classification of retinal images. In this system, U-net model are used for extracted important features such as optical disk which are fed as input in to dense-net model which classified the optic disk as normal or papilledema. Jabber et al. [27] proposed VGG net based triage system for retinal image classification. This system used transfer learning approach and provided accuracy up to 96%.

El-Hug et al. [28] proposed triage system using convolutional neural network model for retinal image classification. In this system, instead of images as input, different features of images are extracted from the images and then feed to CNN model for classification of images as normal or abnormal. Iqbal et al. [29] gives current research trends for retinal image classification. Also, authors give advantages and disadvantages of different triage system for retinal image classification. Zhang et al. [30] proposed hybrid graph convolutional network (HGCM) for retinal image classification. This network based on semi-supervised learning and designs a modularity-based graph learning and integrates convolutional neural network (CNN) features to give graph convolutional network. Abbood et al. [31] proposed deep learning model for retinal image enhancement. This model enhances quality of fundus retinal image before fed into triage system. Liu et al. [32] proposed deep learning model for feature extraction of retinal images before fed into triage system.

Kamran et al. [33] proposed generative adversarial network (GAN) for generation of synthesis retinal fundus images and predication of eye disease using these types of images. This proposed system has the advantages of addressing the problem of imaging retinal vasculature in a non-invasive manner. Latha et al. [34] proposed machine learning based triage system for retinal image classification. In this system, authors used various ML classifiers such as support vector machine, neural network, and adaptive neuro fuzzy inference system. Al-Antary et al. [35] proposed multi-scale attention network for retinal image classification. In this network, the input retinal images are pre-processing using min-pooling filtering method.

Ramasamy et al. [36] machine learning base triage system for retinal image classification. In this system, first, the various textural features such as co-occurrence, run-length matrix and ridgelet coefficients of images are extracted. Then based on these features, the sequential minimal optimization (SMO) based classifier used to classify retinal images. Shi et al. [37] proposed transfer net ResNet50 deep network for automatic retinal image analysis. Nazir et al. [38] proposed deep learning-based system for retinal image classification. In this system, DenseNet-100 used for feature extraction while CenterNet used

for localization and classification of retinal images. Neto et al. [39] analyzed various transfer learning model such as Xception, ResNet152 V2 and Inception ResNet V2 for retinal image classification. Sikder et al. [40] proposed ensemble learning based model for retinal image classification. Bilal et al. [41] proposed deep learning-based model for retinal image classification.

After extensive survey of related papers, it is observed that the existing screening system for glaucoma, used a variety of datasets for performance verification, used a combination of features and machine learning techniques. Survey also indicated that many existing AI based triage systems are based on deep learning and transfer learning-based approaches for retinal image classification. But these systems could achieve maximum accuracy of 97%. Therefore, in this paper, we proposed new AI based screening system which explore advantages of machine learning and deep learning to achieve better performance in term of classification accuracy.

The novel contribution of this paper is a fast, fully automated, and accurate glaucoma screening system that can be used for automated classifying for glaucomatous retinal images for a given dataset. This paper also makes three major contributions to retinal image classification such as (1) Proposed dual learning-based approach which combines deep learning and machine learning. (2) Used deep neural network to obtained deep features for classifying of retinal images. (3) Proposed hybrid classification method that improves the accuracy of classification of glaucomatous retinal images. (4) Overcomes the limitation of existing glaucomatous screening systems [6,11,14,16,24,27,34].

The organization of this paper is as follows. In Section 2, the functionalities of the deep neural network and various classifiers are explained. Section 3 describes each step of the proposed system. Results regarding the performance of the proposed system described in Section 4 followed by concluding the discussion in Section 5.

2. Background

In this section, the information of various terminologies used in the proposed system is discussed.

2.1. Deep neural network (DNN)

The first neural network (NN) was introduced by Dr. Robert Hecht-Nielsen who was the inventor of first neurocomputers [42]. This network basically is known as an artificial neural network (ANN) and is defined as “a computing system made up of a number of simple, highly interconnected processing elements which process information by their dynamic state response to external inputs” [42,43]. This network, also referred to as forwarding neural network (FNN) is used in applications such as big data analysis, person recognition, and data prediction. A simple model for the neural network is shown in Fig. 1. The network has mainly three layers: input layer, hidden layer, and the output layer. The number of neurons or nodes is depended on the size of inputs and outputs. Each node is fully connected to its adjacent layers. The nodes of each adjacent layer are connected by a link carrying specific weight. The working of each node in the neural network is given in Fig. 2.

The neural network is unable to learn weights for unstructured data such as images and videos [44–46]. Therefore, activation functions such as sigmoid and ReLU (rectified linear unit) are used with the neural network. The bias is used for shifting of activation function for better prediction of data. The output of this model (seen in Figs. 1 and 2) can be given by the below Eqs. ((1) & (2)):

$$y = p + b \quad (1)$$

Where,

$$p = W_1 \times x_1 + W_2 \times x_2 + \dots + W_N \times x_N \quad (2)$$

In Eqs. ((1) & (2)), y is predicted output value, W is a weight values of each node and x is input values, and b is a bias.

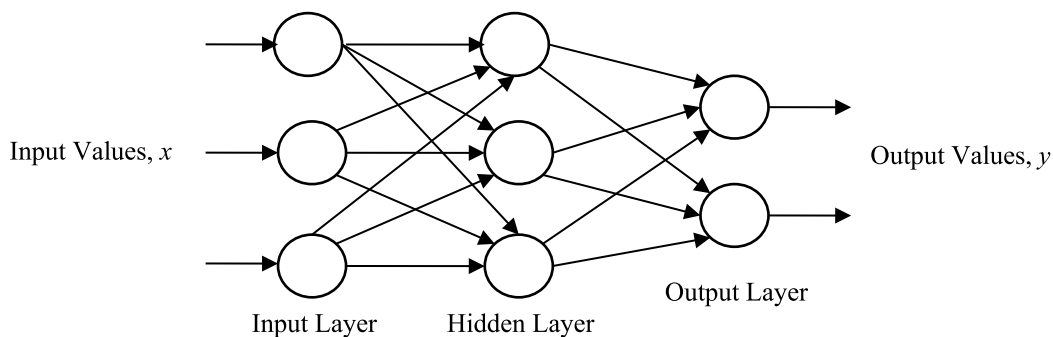


Fig. 1. Basic structure of neural network (NN).

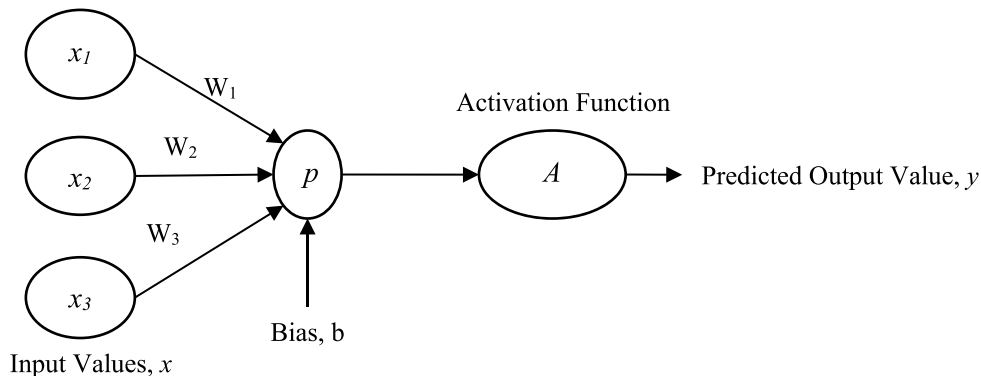


Fig. 2. Working of neural network (NN).

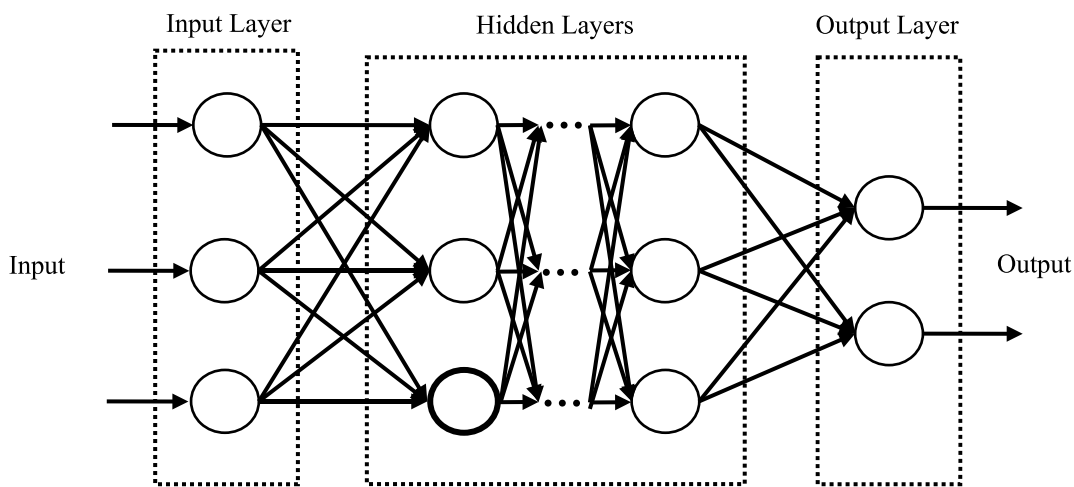


Fig. 3. Basic structure of deep neural network (DNN).

A deep neural network (DNN) is an extension of the neural network. The deep neural network consists of an input layer, several hidden layers, and an output layer. Here, each layer is connected via nodes where each hidden layer gives predicted results based on a prediction of the previous layer. The main difference between NN and DNN is that NN has one hidden layer while DNN has two or more than two hidden layers. The basic structure of DNN is given in Fig. 3.

2.2. Classifier based on machine learning algorithm

Once deep features of each retinal image are obtained using DNN, classification of each image is done using six different types of machine learning algorithms: k-nearest neighbor (kNN), decision tree (DT), support vector machine (SVM), random forest (RF), naive bayes (NB) and logistic regression (LR) and are analyzed for their performance.

3. Proposed system

In the proposed automated system, the color retinal images are taken from the given dataset. After that, three stages are performed for screening of glaucomatous retinal image. The block diagram of the proposed system is shown in Fig. 4 and the working stages of the system are described below.

This proposed system presents new learning model for classification of retinal image classification. This model uses both type of learning such as deep and machine in this. The input of model is color fundus retinal image and output of model is prediction tumor type of input image such as normal and glaucoma. In this model, the deep learning uses for finding important features from the input image. These features of image are then fed to binary classifier for prediction of class of it.

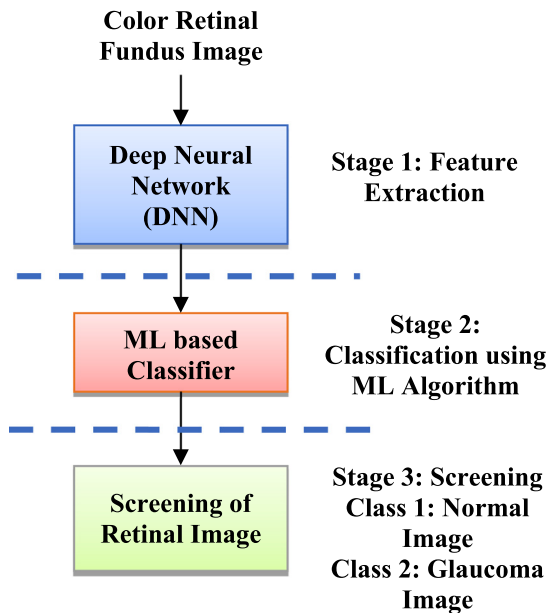


Fig. 4. Block diagram of proposed system.

Here, convolutional layers of SqueezeNet [47] are used for extraction of features from the fundus retinal image while different machine learning algorithm [48] such as k-nearest neighbor (kNN), decision tree (DT), support vector machine (SVM), random forest (RF), naive bayes (NB) and logistic regression (LR) are used for prediction of tumor class. Therefore, this model is called as “dual learning model” and shown in below Fig. 5. The working of this model is described in subsections.

3.1. Feature extraction using SqueezeNet model

SqueezeNet model is a deep convolutional neural network (CNN) which has compressed architecture, small number of parameters and achieved higher accuracy compared to AlexNet and ImageNet with same number of parameters. The main advantages of this model are required less communication channel requires for training, easy to deploy on cloud server and can be customized and used on hardware with limited memory. This original SqueezeNet model [47] has 14 layers where contains 2 conventional convolution layers, 8 fire layers, 3 max pooling layers, 1 global average pooling layer and softmax. Here, we have used only convolution layers of the model for extraction of features from the input color fundus retinal image.

This sequential model starts with a standalone convolution layer followed by 8 fire modules and ending with a final convolution layer. The number of filters per fire module is gradually increased from the beginning to the end of the model. The max pooling with a stride of 2 is performed after layers conv layer 1, fire3, fire7 and conv layer 2. The fire module is a squeeze convolution layer which has only 1×1 filters feeding into an expand layer that has a mix of 1×1 and 3×3 convolution filters. There are three tunable hyperparameters such as $s1 \times 1$, $e1 \times 1$, and $e3 \times 3$. The $s1 \times 1$ refers as squeeze layer with filter size 1×1 while $e1 \times 1$ and $e3 \times 3$ refers as expand layer with filter size 1×1 and 3×3 , respectively. In this model, we use fire modules with hyperparameter $s1 \times 1$ which squeeze layer helps to limit the no. of input channels to the 3×3 filters. After extract features from the input retinal fundus image, we used to flatten layer which converts features into one dimensional layer.

3.2. ML based binary classifier

In machine learning, multiclass classification refers the problem of classifying instances into one of three or more classes. In this case, we

need to classified input retinal fundus image into one of class such as no tumor, glioma tumor, meningioma tumor and pituitary tumor. For this purpose, in this model, we have used different conventional classifiers such as k nearest neighbor (KNN), support vector machine (SVM), Decision Tree (DT), Naïve Bayes (NB), and logistic regression (LR) for classification of multiclass brain tumor images. Here, we have modified each classifier which performs the operation of multiclass classification and prediction.

4. Results

The performance of the classifiers and screening of glaucomatous retinal image are analyzed in this section. The metrics used for performance analysis of system are confusion matrix, true positive (TP), true negative (TN), false positive (FP) and false negative (FN) [48]. The confusion matrix for the proposed system is given in Fig. 6.

- **True Positive (TP):** A glaucoma retinal image if predicted by classifier as glaucoma retinal image.
- **True Negative (TN):** A normal retinal image if predicted as normal retinal image.
- **False Positive (FP):** A normal retinal image if classified as glaucoma retinal image.
- **False Negative (FN):** A glaucoma retinal image if predicted as normal retinal image.

Other performance metrics such as Classifier accuracy (CA), Precision, Recall (sensitivity) and F1 score are calculated using below Eqs. ((3) to (6)) based on the above parameters.

$$CA = \frac{TP + TN}{TP + FP + TN + FN} \quad (3)$$

$$P = \frac{TP}{TP + FP} \quad (4)$$

$$R = \frac{TP}{TP + FN} \quad (5)$$

$$F1 = \frac{2 \times P \times R}{P + R} \quad (6)$$

The main objective of the proposed system is to classify the input fundus retinal image that is a glaucomatous image or a normal image. Here, the system is designed and validated with 2-fold cross validation method. Here, the system is designed and validated with a 2-fold cross validation method. The size of training dataset is 101 retinal images and test dataset is 30 retinal images.

For training of proposed system, the hyper parameters values such as batch size, epochs and learning rate is chosen as 32, 10 and 0.001, respectively using try and error method. The adaptive moment estimation (Adam) optimizer and ReLU activation function is used in the proposed system.

The following subsections present the dataset used for the analysis of the system, features of the dataset, and the performance of the classifier on given features of dataset and comparison with existing work.

4.1. Performance of proposed system using DRISTHI-GS dataset

4.1.1. Information of DRISTHI-GS dataset

The DRISTHI-GS dataset was created by IIIT, Hyderabad [49] and is used in the simulations. The retinal images in the dataset are obtained by Aravind Eye Hospital, Madurai, India. This dataset has a total of 101 images in which 70 images are the glaucomatous image and 31 images are normal images. The images belong to patients with age group between 40 to 80 years. The sample retinal images from this dataset are given in Fig. 7.

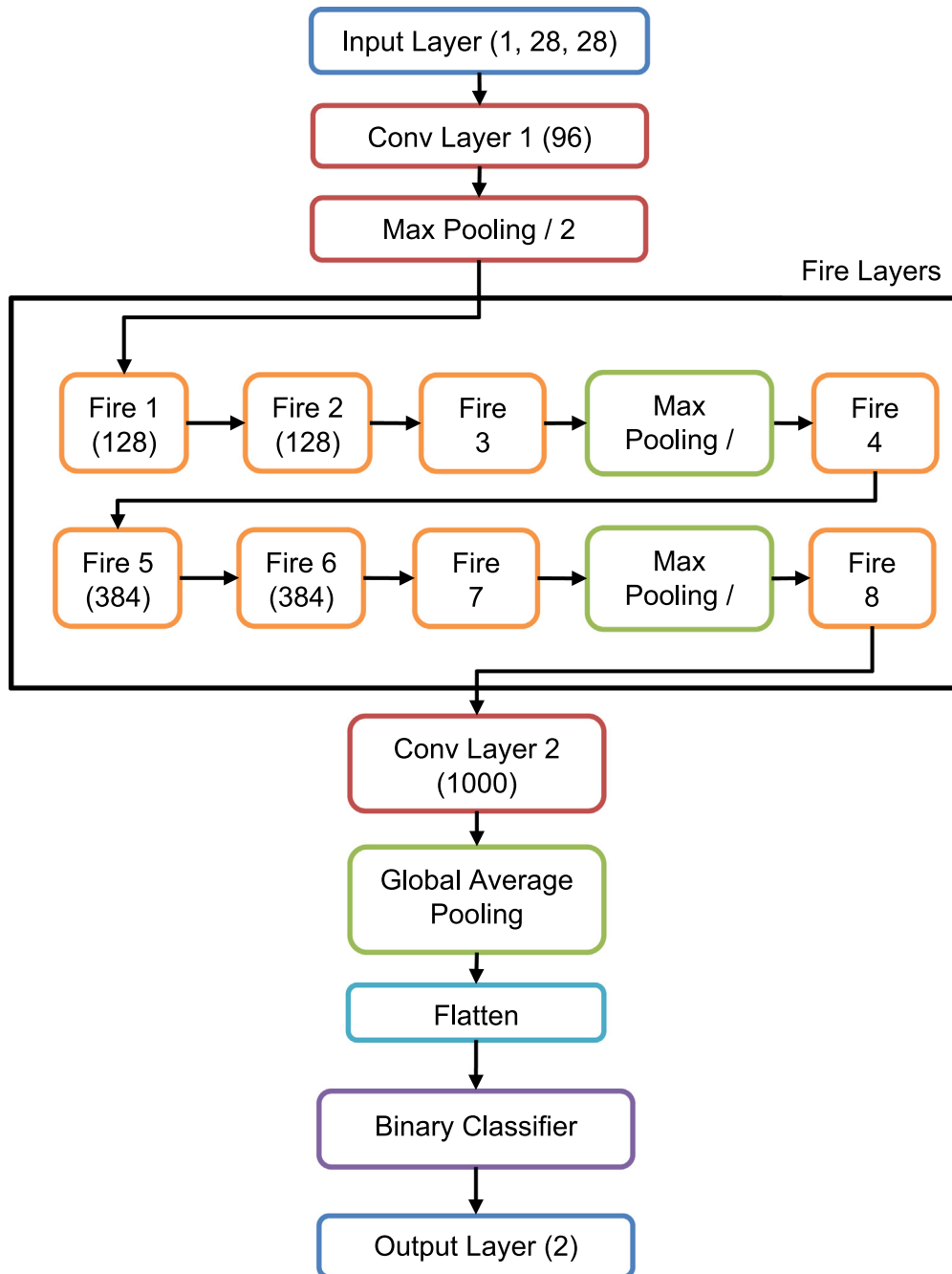


Fig. 5. Dual learning model for retinal image classification.

4.1.2. Features for DRISTHI-GS dataset

In the proposed system, SqueezeNet model is used to extract deep features from retinal images. The deep features of the first seven layers (n0–n6) are shown in Table 1 along with the height and width of the image.

4.1.3. Performance evaluation of classifiers using DRISTHI-GS dataset

After obtaining deep features of the retinal image, the features are fed to 6 different classifiers for, and the performance analysis of each classifier is done. The classifiers applied are kNN, decision tree (DT), SVM, naïve bayes (NB), random forest (RF) and logistic regression (LR). The confusion matrices obtained for the given dataset for these classifiers are given in Table 2. The results indicate that the performance of LR classifier is better than other classifiers in term of

accuracy, sensitivity, and precision for classification of glaucomatous retinal images.

The testing of the proposed system is done using high resolution fundus (HRF) retinal images dataset [50]. This database contains 15 glaucomatous retinal images and 15 normal retinal images. The performance results of proposed system for predication of glaucomatous retinal images and normal retinal images are given in Table 3. The results in table show that this proposed system successfully distinguishes and predicated these two types of retinal images.

4.2. Performance of proposed system using ORIGA dataset

4.2.1. Information of ORIGA dataset

ORIGA dataset was created by trained professionals from Singapore eye research institute [51]. This dataset has a total 650 images in

Table 1
Deep features for proposed system.

Image category	Width	Height	n0	n1	n2	n3	n4	n5	n6
Glaucoma_1	2049	1751	0.000	0.027	0.000	0.000	0.000	0.000	0.534
Glaucoma_2	2045	1752	0.000	1.455	0.000	0.000	0.000	0.000	0.968
Glaucoma_3	2047	1759	0.000	1.016	0.000	0.000	0.000	0.314	0.900
Glaucoma_4	2049	1762	0.000	0.571	0.000	0.000	0.000	0.000	0.000
Normal_1	2049	1757	0.000	0.000	0.000	0.000	0.000	0.000	0.000
Normal_2	2049	1755	0.000	0.867	0.000	0.000	0.000	1.073	0.000
Normal_3	2048	1754	0.000	2.191	0.000	0.000	0.000	0.654	0.000
Normal_4	2463	1759	0.000	0.000	0.000	0.000	0.000	0.000	0.888

Table 2
Training performance matrices of proposed system using DRISTHI-GS dataset.

Classifier	Confusion matrix	Area Under Curve (AUC)	Classifier Accuracy (CA)	F1	Precision	Recall
kNN	$\begin{bmatrix} 70 & 0 \\ 21 & 10 \end{bmatrix}$	0.942	0.792	0.870	0.769	1.000
Decision Tree	$\begin{bmatrix} 69 & 1 \\ 3 & 28 \end{bmatrix}$	0.996	0.960	0.972	0.958	0.986
SVM	$\begin{bmatrix} 70 & 0 \\ 27 & 4 \end{bmatrix}$	0.946	0.733	0.838	0.722	1.000
Random Forest	$\begin{bmatrix} 69 & 1 \\ 4 & 27 \end{bmatrix}$	0.995	0.950	0.965	0.945	0.986
Naïve Bayes	$\begin{bmatrix} 38 & 32 \\ 3 & 28 \end{bmatrix}$	0.836	0.653	0.685	0.927	0.543
Logistic Regression	$\begin{bmatrix} 70 & 0 \\ 1 & 30 \end{bmatrix}$	1.000	0.990	0.993	0.986	1.000

Table 3
Testing performance matrices of proposed system using HRF dataset.

Classifier	Confusion matrix	Classifier Accuracy (CA)	F1	Precision	Recall
kNN, Decision Tree, SVM, Random Forest, Logistic Regression	$\begin{bmatrix} 15 & 0 \\ 15 & 0 \end{bmatrix}$	0.500	0.333	0.250	0.500
Naïve Bayes	$\begin{bmatrix} 3 & 12 \\ 2 & 13 \end{bmatrix}$	0.533	0.475	0.560	0.533

		Predicted	
		Glaucoma	Normal
Actual	Glaucoma	TP	FP
	Normal	FN	TN

Fig. 6. Confusion matrix for proposed system.

which 168 images are the glaucomatous image and 482 images are normal images. For performance analysis of proposed system, we split whole dataset into training dataset (80%) and testing dataset (20%). The sample retinal images from this dataset are given in Fig. 8.

4.2.2. Performance evaluation of classifiers using ORIGA dataset

The confusion matrices obtained for the ORIGA dataset for various machine learning classifiers are given in Table 4. The results indicate that the performance of LR classifier is better than other classifiers in term of accuracy, sensitivity, and precision for classification of glaucomatous retinal images. The performance results of proposed system for predication of glaucomatous retinal images and normal retinal images using testing dataset are given in Table 5. The results in table show that

this proposed system successfully distinguishes and predicated these two types of retinal images.

4.3. Comparison with existing work

A comparison of the proposed triage system for classifying glaucomatous retinal image with the existing triage systems is given in Table 6. Most of the existing systems tested their methods on 50/101 images of DRISTHI-GS dataset, and have used texture features, CDR features, and hybrid features. The comparison of systems is performed using various parameters such as AUC, recall, precision, F1 and accuracy. This is shows that proposed system classified input color fundus image in correct way.

The effectiveness the various features is also compared with existing triage systems in Table 7. The existing systems are used features like texture, cup to disk ratio, hybrid features while proposed system used deep features for classifying retinal images and resulted in better accuracy and performance than existing systems for classifying glaucomatous retinal images. Also, the maximum training accuracy achieved in existing system is around 0.990 while proposed system provides maximum training accuracy up to 1.000.

5. Conclusion

In this paper, a deep neural network and machine learning based computer-aided system for classification of the glaucomatous retinal image is proposed. Here, 512 deep features of retinal images are explored using DNN. The proposed system tested and analyzed all images from the public datasets such as DRISTHI-GS1 and ORIGA. The classification of the glaucomatous retinal image is performed using

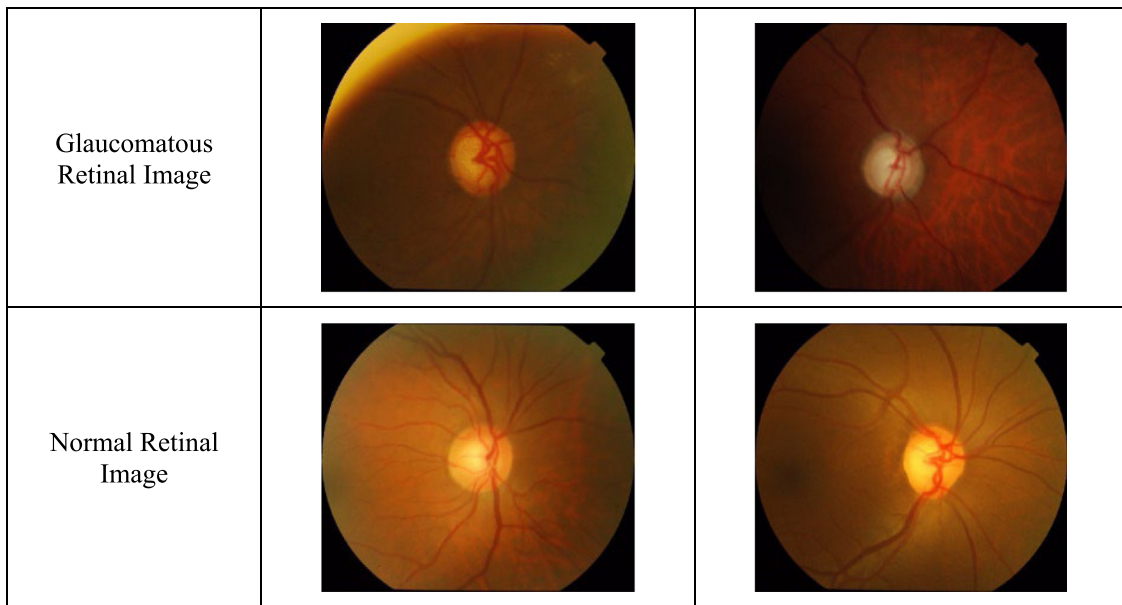


Fig. 7. Sample retinal images from DRISTHI-GS dataset.

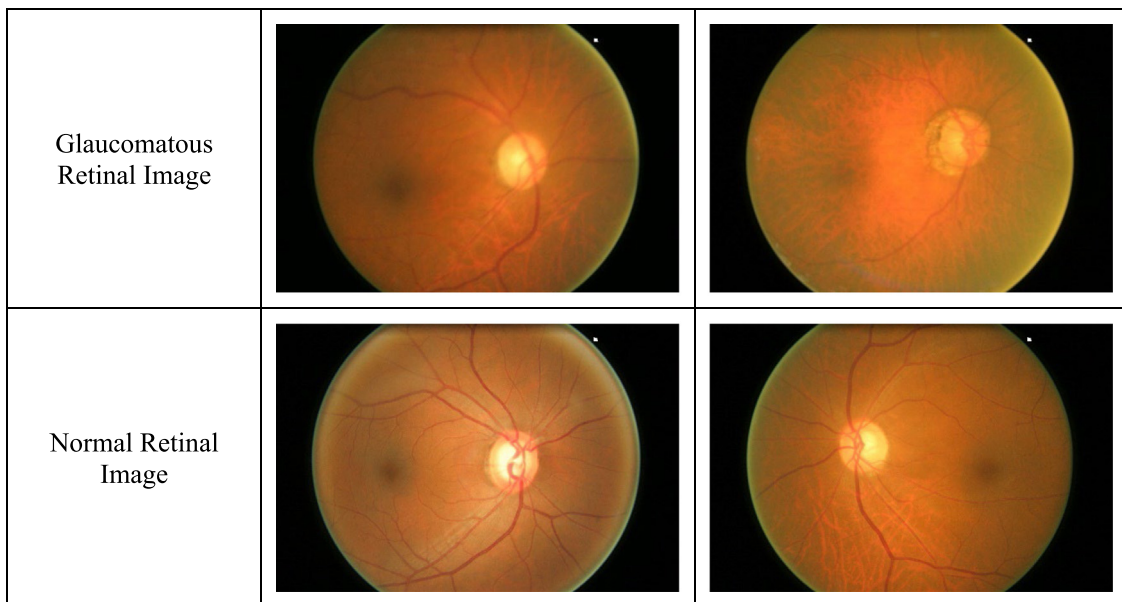


Fig. 8. Sample retinal images from ORIGA dataset.

Table 4
Performance matrices of proposed system using ORIGA training dataset.

Classifier	Confusion matrix	Area Under Curve (AUC)	Classifier Accuracy (CA)	F1	Precision	Recall
kNN	$\begin{bmatrix} 73 & 62 \\ 32 & 353 \end{bmatrix}$	0.894	0.819	0.811	0.810	0.819
Decision Tree	$\begin{bmatrix} 133 & 2 \\ 4 & 381 \end{bmatrix}$	0.998	0.988	0.988	0.989	0.988
SVM	$\begin{bmatrix} 92 & 43 \\ 10 & 375 \end{bmatrix}$	0.947	0.898	0.893	0.898	0.898
Naïve Bayes	$\begin{bmatrix} 90 & 45 \\ 114 & 271 \end{bmatrix}$	0.735	0.694	0.710	0.749	0.694
Logistic Regression	$\begin{bmatrix} 132 & 3 \\ 0 & 385 \end{bmatrix}$	1.000	0.994	0.994	0.994	0.994

Table 5
Performance matrices of proposed system using ORIGA testing dataset.

Classifier	Confusion matrix	Area Under Curve (AUC)	Classifier Accuracy (CA)	F1	Precision	Recall
kNN	$\begin{bmatrix} 7 & 26 \\ 16 & 81 \end{bmatrix}$	0.598	0.677	0.656	0.642	0.677
Decision Tree	$\begin{bmatrix} 11 & 22 \\ 24 & 73 \end{bmatrix}$	0.558	0.646	0.650	0.653	0.646
SVM	$\begin{bmatrix} 9 & 24 \\ 7 & 90 \end{bmatrix}$	0.661	0.762	0.730	0.732	0.762
Naïve Bayes	$\begin{bmatrix} 23 & 10 \\ 38 & 59 \end{bmatrix}$	0.697	0.631	0.655	0.734	0.631
Logistic Regression	$\begin{bmatrix} 14 & 19 \\ 26 & 71 \end{bmatrix}$	0.610	0.654	0.664	0.677	0.654

Table 6
Performance comparison of various triage system for retinal image classification.

Triage System	Classifiers	AUC	Recall	Precision	F1	Accuracy
Claro (2016) et al. [6]	MLP, RC, RF and SVM-RBF	NR	0.835 to 0.930	0.827 to 0.930	0.827 to 0.929	0.835 to 0.930
Zou (2018) et al. [16]	SVM, RF	0.732, 0.733	NR	NR	NR	0.74, 0.78
Goel (2021) et al. [24]	CNN	0.831 to 0.997	0.773 to 0.969	0.571 to 0.963	0.706 to 0.912	0.885 to 0.959
Jabbar (2022) et al. [27]	ResNet, GoogleNet, AlexNet and VGGNet	0.924 to 0.971	0.854 to 0.953	0.937 to 0.990	0.918 to 0.967	0.924 to 0.966
Latha (2022) et al. [34]	ANFIS	NR	0.963	0.961	NR	0.962
Proposed	kNN, SVM, DT, RF, NB and LR	0.836 to 1.000	0.543 to 1.000	0.722 to 0.986	0.838 to 0.993	0.653 to 0.990

NR = Not Reported

Table 7
Comparison of various features of different Triage systems.

System	Features	Classifiers	Image dataset	No. of images	Maximum training accuracy
Claro (2016) et al. [6]	Texture	MLP, RC, RF, and SVM-RBF	DRISTHI-GS	50	0.930
Sevastopolsky (2017) et al. [11]	Cup to Disk Ratio (CDR)	NN	DRISTHI-GS	50	NR
Nawaldgi (2018) et al. [14]	Cup to Disk Ratio (CDR)	Adaptive Thresholding	DRISTHI-GS	101	0.990
Zou (2018) et al. [16]	Hybrid Features	SVM and RF	DRISTHI-GS	101	0.780
Proposed	Deep Features	kNN, SVM, DT, RF, NB, and LR	DRISTHI-GS	101	1.000

six machine learning-based classifiers: kNN, SVM, DT, RF, NB, and LR. It is observed that the combination of DNN with LR based machine learning-based classifier outperforms all existing glaucomatous screening systems, with improvement in classification accuracy and sensitivity.

Future work will be focused on the assessment of deep learning-based classifier combination for classification of glaucomatous retinal images. The work may also focus on detection and screening of vascular bleeding in the retina due to macular degeneration and diabetic retinopathy (DR) using machine learning techniques. Also, experimental results particularly F1 score indicates that proposed system need to test with more balance dataset to improve this score and acceptance for practical implementation in future.

Funding

None

Declaration of competing interest

The authors declare that they have no known competing financial interests or personal relationships that could have appeared to influence the work reported in this paper.

Data availability

The authors do not have permission to share data.

Acknowledgments

None

References

- [1] Priority Eye Disease, 2019. Web link: <https://www.who.int/blindness/causes/priority/en/>. Last Access: February 2019.
- [2] K. Manju, RS. Sabeenian, Robust cdr calculation for glaucoma identification, Special Issue Biomed. Res. 2018 (2018) S137–S144.
- [3] R. Bock, J. Meier, L.G. Nyúl, J. Hornegger, G. Michelson, Glaucoma risk index: automated glaucoma detection from color fundus images, Med. Image Anal. 14 (3) (2010) 471–481.
- [4] D. Shriranjani, S.G. Tebby, S.C. Satapathy, N. Dey, V. Rajinikanth, Kapur's entropy and active contour-based segmentation and analysis of retinal optic disc, in: Computational Signal Processing and Analysis, Springer, Singapore, 2018 pp. 287–295.
- [5] A. Ghosh, A. Sarkar, A.S. Ashour, D. Balas-Timar, N. Dey, V.E. Balas, Grid color moment features in glaucoma classification, Int. J. Adv. Comput. Sci. Appl. 6 (9) (2015) 1–14.

- [6] M. Claro, L. Santos, W. Silva, F. Araújo, N. Moura, A. Macedo, Automatic glaucoma detection based on optic disc segmentation and texture feature extraction, *CLEI Electr. J.* 19 (2) (2016) 5.
- [7] A. Soman, D. Mathew, Glaucoma detection and segmentation using retinal images, *Int. J. Sci. Eng. Technol. Res.* 5 (5) (2016) 1346–1350.
- [8] A. Dey, S.K. Bandyopadhyay, Automated glaucoma detection using support vector machine classification method, *Br. J. Med. Med. Res.* 11 (12) (2016) 1–12.
- [9] S. Maheshwari, R.B. Pachori, U.R. Acharya, Automated diagnosis of glaucoma using empirical wavelet transform and correntropy features extracted from fundus images, *IEEE J. Biomed. Health Inf.* 21 (3) (2017) 803–813.
- [10] P. Singh, B. Marakarkandy, Comparative study of glaucoma detection using different classifiers, *Int. J. Electron. Electr. Comput. Syst.* 6 (7) (2017) 223–232.
- [11] A. Sevastopolsky, Optic disc and cup segmentation methods for glaucoma detection with modification of U-Net convolutional neural network, *Pattern Recognit. Image Anal.* 27 (3) (2017) 618–624.
- [12] D. Sarkar, S. Das, Automated Glaucoma detection of medical image using biogeography-based optimization, in: *Advances in Optical Science and Engineering*, Springer, Singapore, 2017, pp. 381–388.
- [13] A. Dey, K.N. Dey, Automated glaucoma detection from fundus images of eye using statistical feature extraction methods and support vector machine classification, in: *Industry Interactive Innovations in Science, Engineering, and Technology*, Springer, Singapore, 2018, pp. 511–521.
- [14] S. Nawaldgi, Y.S. Lalitha, M. Reddy, A novel adaptive threshold and isnt rule based automatic glaucoma detection from color fundus images, in: *Data Engineering and Intelligent Computing*, Springer, Singapore, 2018, pp. 139–147.
- [15] A. Septiarni, D.M. Khairina, A.H. Kridalaksana, H. Hamdani, Automatic glaucoma detection method applying a statistical approach to fundus images, *Healthcare Inform. Res.* 24 (1) (2018) 53–60.
- [16] B. Zou, Q. Chen, R. Zhao, P. Ouyang, C. Zhu, X. Duan, An approach for Glaucoma detection based on the features representation in radon domain, in: *International Conference on Intelligent Computing*, Springer, Cham, 2018, pp. 259–264.
- [17] M.Y. Yip, G. Lim, Z.W. Lim, Q.D. Nguyen, C.C. Chong, M. Yu, et al., Technical and imaging factors influencing performance of deep learning systems for diabetic retinopathy, *NPJ Digit. Med.* 3 (1) (2020) 1–12.
- [18] J. Sahlsten, J. Jaskari, J. Kivinen, L. Turunen, E. Jaanio, K. Hietala, K. Kaski, Deep learning fundus image analysis for diabetic retinopathy and macular edema grading, *Sci. Rep.* 9 (1) (2019) 1–11.
- [19] P.N. Schacknow, J.R. Samples, *The Glaucoma Book: a Practical, Evidence-Based Approach to Patient Care*, Springer Science & Business Media, 2010.
- [20] S. Das, C. Malathy, Survey on the diagnosis of diseases from retinal images, *J. Phys. Conf. Ser.* 1000 (1) (2018) 012053.
- [21] J. Wang, G. Deng, W. Li, Y. Chen, F. Gao, H. Liu, et al., Deep learning for quality assessment of retinal OCT images, *Biomed. Opt. Express* 10 (12) (2019) 6057–6072.
- [22] I.K. Gupta, A. Choubey, S. Choubey, Mayfly optimization with deep learning enabled retinal fundus image classification model, *Comput. Electr. Eng.* 102 (2022) 108176.
- [23] L. Abdel-Hamid, Retinal image quality assessment using transfer learning: Spatial images vs. wavelet detail subbands, *Ain Shams Eng. J.* 12 (3) (2021) 2799–2807.
- [24] S. Goel, S. Gupta, A. Panwar, S. Kumar, M. Verma, S. Bourouis, M.A. Ullah, Deep learning approach for stages of severity classification in diabetic retinopathy using color fundus retinal images, *Math. Probl. Eng.* 2021 (2021).
- [25] J. Kaur, P. Kaur, Automated computer-aided diagnosis of diabetic retinopathy based on segmentation and classification using K-nearest neighbor algorithm in retinal images, *Comput. J.* (2022).
- [26] T. Saba, S. Akbar, H. Kolivand, S. Ali Bahaj, Automatic detection of papilledema through fundus retinal images using deep learning, *Microsc. Res. Tech.* 84 (12) (2021) 3066–3077.
- [27] M.K. Jabbar, J. Yan, H. Xu, Z. Ur Rehman, A. Jabbar, Transfer learning-based model for diabetic retinopathy diagnosis using retinal images, *Brain Sci.* 12 (5) (2022) 535.
- [28] N.A. El-Hag, A. Sedik, W. El-Shafai, H.M. El-Hoseny, A.A. Khalaf, A.S. El-Fishawy, et al., Classification of retinal images based on convolutional neural network, *Microsc. Res. Tech.* 84 (3) (2021) 394–414.
- [29] S. Iqbal, T.M. Khan, K. Naveed, S.S. Naqvi, S.J. Nawaz, Recent trends and advances in fundus image analysis: A review, *Comput. Biol. Med.* (2022) 106277.
- [30] G. Zhang, J. Pan, Z. Zhang, H. Zhang, C. Xing, B. Sun, M. Li, Hybrid graph convolutional network for semi-supervised retinal image classification, *IEEE Access* 9 (2021) 35778–35789.
- [31] S.H. Abbood, H.N.A. Hamed, M.S.M. Rahim, A. Rehman, T. Saba, S.A. Bahaj, Hybrid retinal image enhancement algorithm for diabetic retinopathy diagnostic using deep learning model, *IEEE Access* 10 (2022) 73079–73086.
- [32] R. Liu, S. Gao, H. Zhang, S. Wang, L. Zhou, J. Liu, MTNet: A combined diagnosis algorithm of vessel segmentation and diabetic retinopathy for retinal images, *PLoS One* 17 (11) (2022) e0278126.
- [33] S.A. Kamran, K.F. Hossain, A. Tavakkoli, S.L. Zuckerbrod, S.A. Baker, Vtgan: Semi-supervised retinal image synthesis and disease prediction using vision transformers, in: *Proceedings of the IEEE/CVF International Conference on Computer Vision*, 2021, pp. 3235–3245.
- [34] G. Latha, P.A. Priya, Glaucoma retinal image detection and classification using machine learning algorithms, *J. Phys. Conf. Ser.* 2335 (1) (2022) 012025.
- [35] M.T. Al-Antary, Y. Arafa, Multi-scale attention network for diabetic retinopathy classification, *IEEE Access* 9 (2021) 54190–54200.
- [36] L.K. Ramasamy, S.G. Padinjappurathu, S. Kadry, R. Damaševičius, Detection of diabetic retinopathy using a fusion of textural and ridgelet features of retinal images and sequential minimal optimization classifier, *PeerJ Comput. Sci.* 7 (2021) e456.
- [37] C. Shi, J. Lee, G. Wang, X. Dou, F. Yuan, B. Zee, Assessment of image quality on color fundus retinal images using the automatic retinal image analysis, *Sci. Rep.* 12 (1) (2022) 1–11.
- [38] T. Nazir, M. Nawaz, J. Rashid, R. Mahum, M. Masood, A. Mehmood, et al., Detection of diabetic eye disease from retinal images using a deep learning based CenterNet model, *Sensors* 21 (16) (2021) 5283.
- [39] A. Neto, J. Camara, A. Cunha, Evaluations of deep learning approaches for Glaucoma screening using retinal images from mobile device, *Sensors* 22 (4) (2022) 1449.
- [40] N. Sikder, M. Masud, A.K. Bairagi, A.S.M. Arif, A.A. Nahid, H.A. Alhummyani, Severity classification of diabetic retinopathy using an ensemble learning algorithm through analyzing retinal images, *Symmetry* 13 (4) (2021) 670.
- [41] A. Bilal, L. Zhu, A. Deng, H. Lu, N. Wu, AI-based automatic detection and classification of diabetic retinopathy using U-Net and deep learning, *Symmetry* 14 (7) (2022) 1427.
- [42] A basic introduction to neural networks, 2018, Website: <http://pages.cs.wisc.edu/~bolo/shipyard/neural/local.html>. Last Access: February 2018.
- [43] Caudill M., *Neural Network Primer: Part I. AI Expert*, 1989.
- [44] T. Hastie, R. Tibshirani, J. Friedman, *The Elements of Statistical Learning: Data Mining, Inference, and Prediction*, Springer Series in Statistics, 2009.
- [45] S. Shalev-Shwartz, S. Ben-David, *Understanding Machine Learning: from Theory to Algorithms*, Cambridge university press, 2014.
- [46] J.J. Almagro Armenteros, C.K. Sønderby, S.K. Sønderby, H. Nielsen, O. Winther, DeepLoc: prediction of protein subcellular localization using deep learning, *Bioinformatics* 33 (21) (2017) 3387–3395.
- [47] F.N. Iandola, S. Han, M.W. Moskewicz, K. Ashraf, W.J. Dally, K. Keutzer, SqueezeNet: AlexNet-level accuracy with 50x fewer parameters and < 0.5 MB model size, 2016, arXiv preprint arXiv:1602.07360.
- [48] S. Borra, R. Thanki, N. Dey, *Satellite Image Analysis: Clustering and Classification*, Springer, Singapore, 2019.
- [49] J. Sivaswamy, S.R. Krishnadas, G.D. Joshi, M. Jain, A.U.S. Tabish, Drishtigs: Retinal image dataset for optic nerve head (onh) segmentation, in: 2014 IEEE 11th International Symposium on Biomedical Imaging, ISBI, IEEE, 2014 pp. 53–56.
- [50] J. Odstreilik, R. Kolar, A. Budai, J. Hornegger, J. Jan, J. Gazarek, et al., Retinal vessel segmentation by improved matched filtering: evaluation on a new high-resolution fundus image database, *IET Image Process.* 7 (4) (2013) 373–383.
- [51] Z. Zhang, F.S. Yin, J. Liu, W.K. Wong, N.M. Tan, B.H. Lee, et al., Origa-light: An online retinal fundus image database for glaucoma analysis and research, in: 2010 Annual International Conference of the IEEE Engineering in Medicine and Biology, IEEE, 2010, pp. 3065–3068.